Supporting information

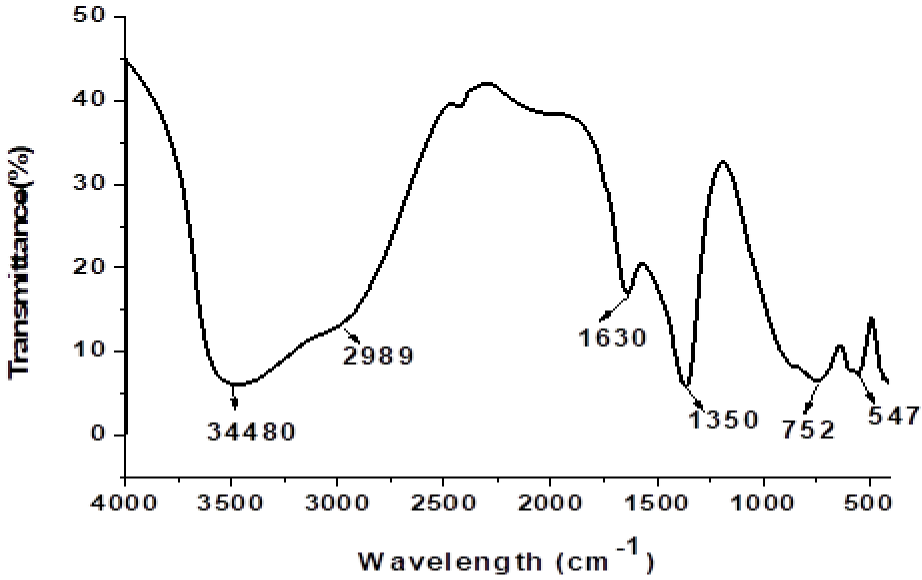

Fig.S$_1$ FTIR of CoAl-31

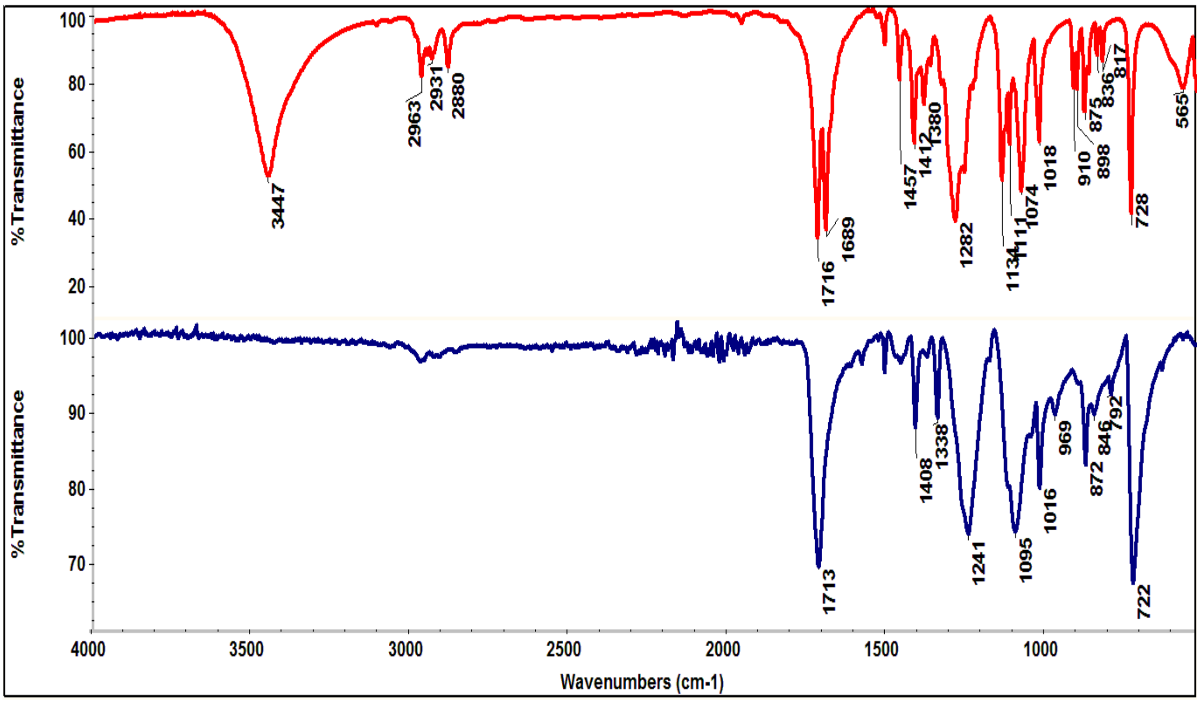

Fig.S$_2$ Overlaid FTIR spectrum of PET (bottom) and BHET (top)

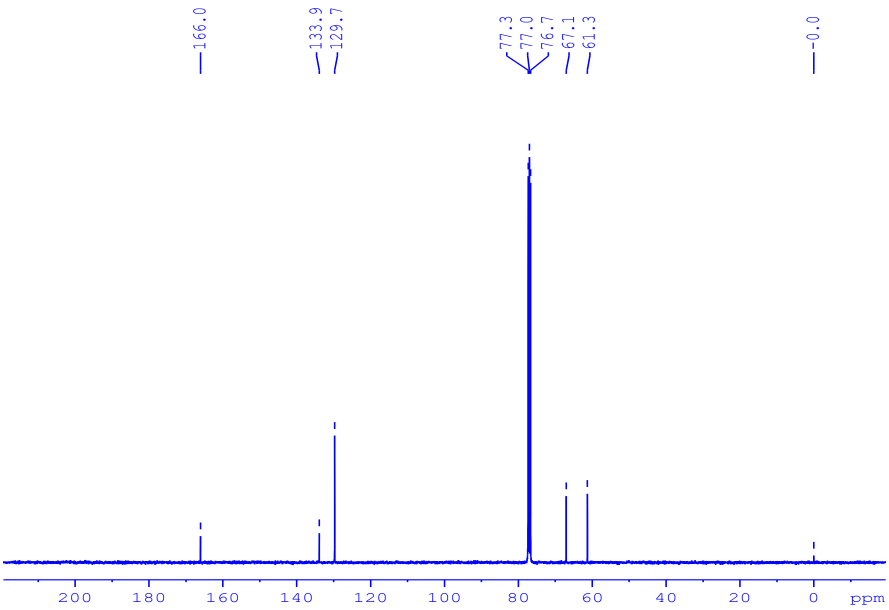

Fig.S3 ^{13}C NMR of BHET

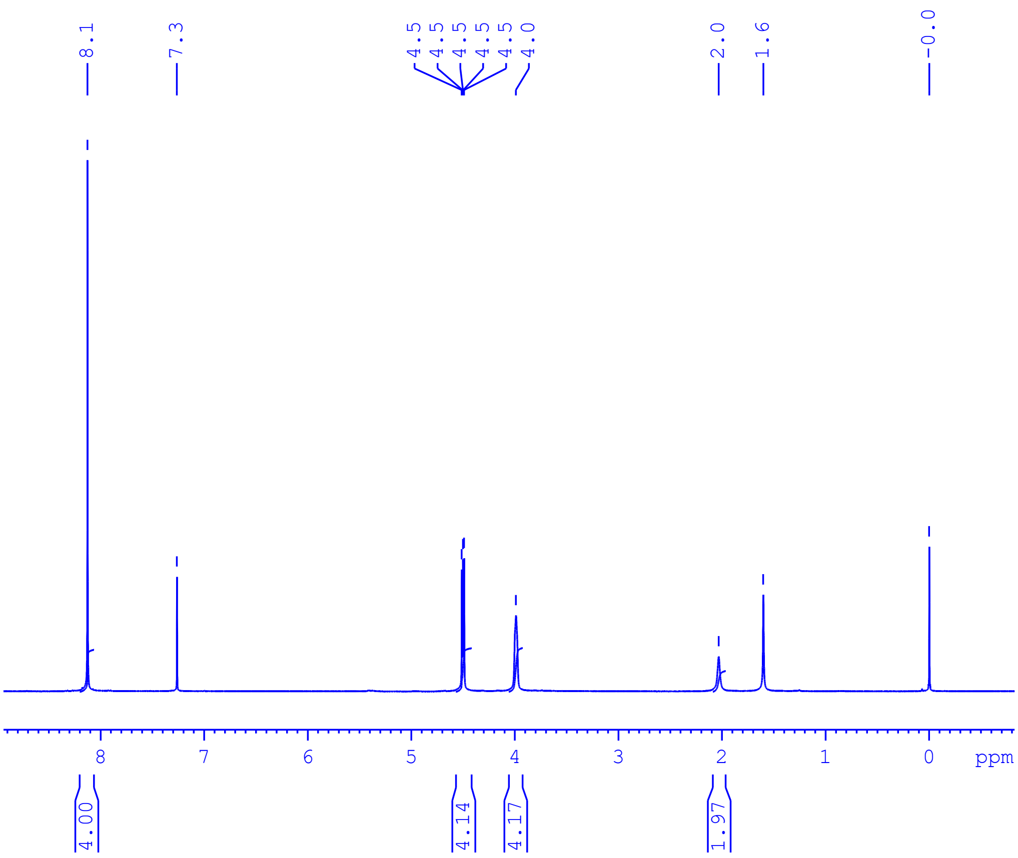

Fig.S4 ^{1}H NMR of BHET

Table.S_1 Properties of Co-Al CO_3 with different Co^{2+}/Al^{3+} ratios

LDH	Experimental Co/Al Ratio	d003(Å)	d110(Å)	a(Å)	c(Å)	Crystalite size(nm)
CO-Al-11	0.8	7.50	1.52	3.04	22.50	13.0
CO-Al-21	1.9	7.53	1.53	3.06	22.59	13.0
CO-Al-31	2.7	7.66	1.54	3.08	22.98	10.4
CO-Al-41	3.6	7.69	1.55	3.10	23.07	9.8

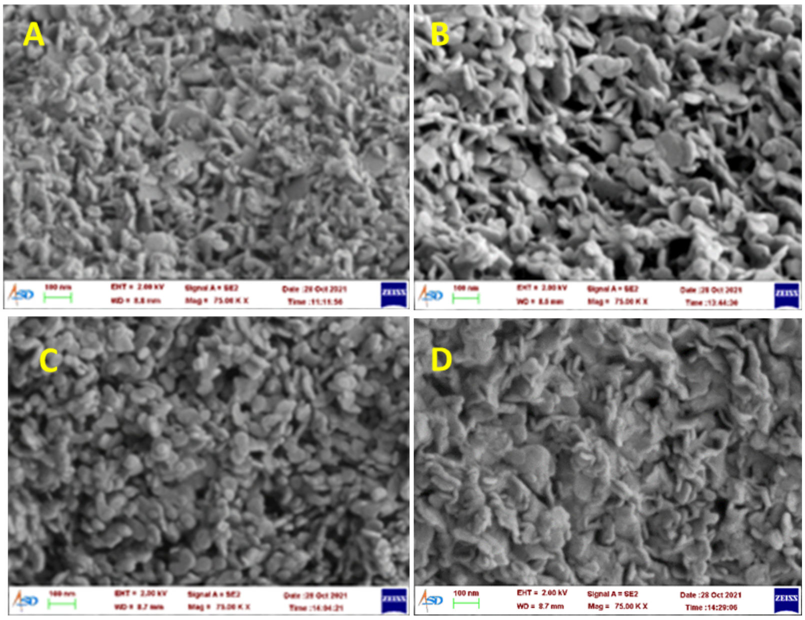

Fig.S_5 FESEM images of Co-Al CO_3 with different Co^{2+}/Al^{3+} ratios (A) ratio 1:1, (B) ratio 2:1, (C) ratio 31 and (D) ratio 4:1

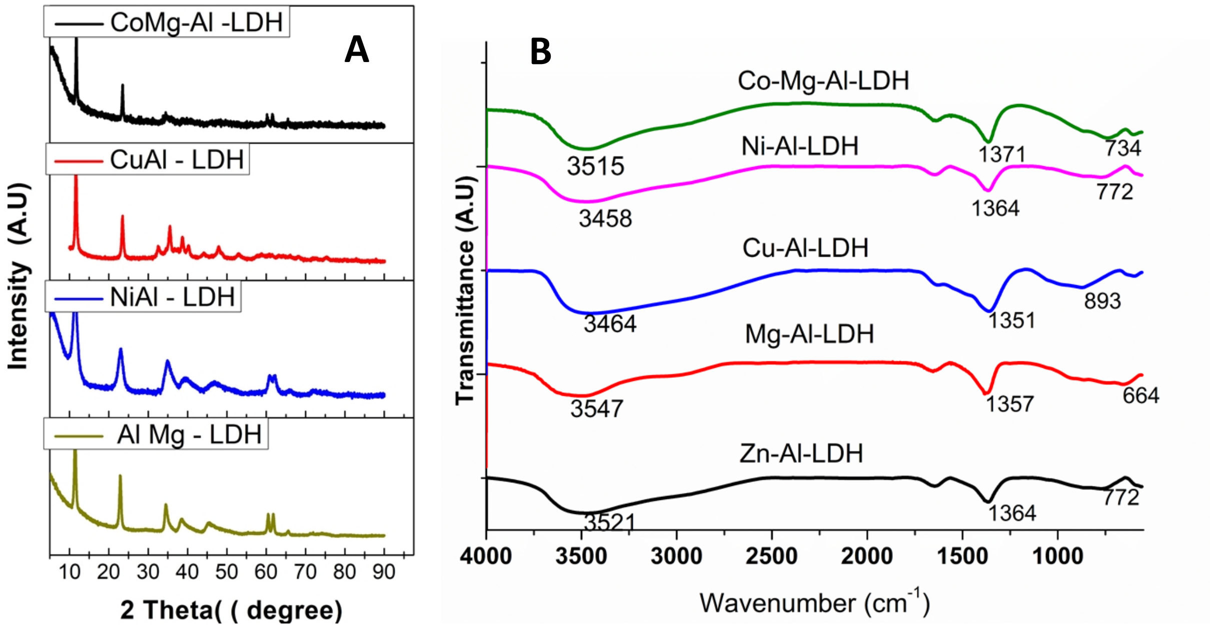

Fig.S6 (A) XRD and (B) FTIR spectra of LDH materials with different M^{2+} cation

Table S_2: Comparison of Cobalt containing catalysts for PET glycolysis

	Catalyst	Temperature (°C)	Time (h)	BHET (%)	Reference
1	Co_3O_4	260	1	63	https://doi.org/10.1016/j.polymdegradstab.2013.01.007
2	$CoCl_2$ (anh) $CoCl_2$ (anh)/dcype CoCl2 (anh)/dppe $CoCl_2$ (anh)/dppf $CoCl_2$ (anh)/BEt3	190	3	65 71 53 31 85	https://doi.org/10.1007/s10562-016-1897-0.
3	Recovered CoO from lithium-ion batteries	196	2	10	https://doi.org/10.1007/s12649-019-00807-6
4	Co NPs	180	3	77	https://doi.org/10.1021/acssuschemeng.8b02294
5	CoRZnO	196	2	80	https://doi.org/10.1007/s12649-019-00807-6
6	rGO\[TESPMI]2CoCl4	190	3	95	https://doi.org/10.1016/j.polymdegradstab.2021.109691

7	$CoMn_2O_4$	260	1	89	https://doi.org/10.1016/j.polymdegradstab.2013.01.007
8	$ZnCo2O_4$	260	1	89	https://doi.org/10.1016/j.polymdegradstab.2013.01.007
9	$CoFe_2O_4$@ZIF-8/ZIF-67	200	1	84	https://doi.org/10.1016/j.fuel.2021.121397
10	CoFe2O4	195	2.5	73	https://doi.org/10.1016/j.eurpolymj.2021.110590
11	CoFe2O4/C10-OAC	195	2.5	96	https://doi.org/10.1016/j.eurpolymj.2021.110590
12	Mechano chemically prepared $CoFe_2O_4$	190	6.0	77	https://doi.org/10.1016/j.cej.2022.137926
13	Co Al 31	180	2	96	This work
13	Co Al 31@Fe_3O_4	180	2	99	This work

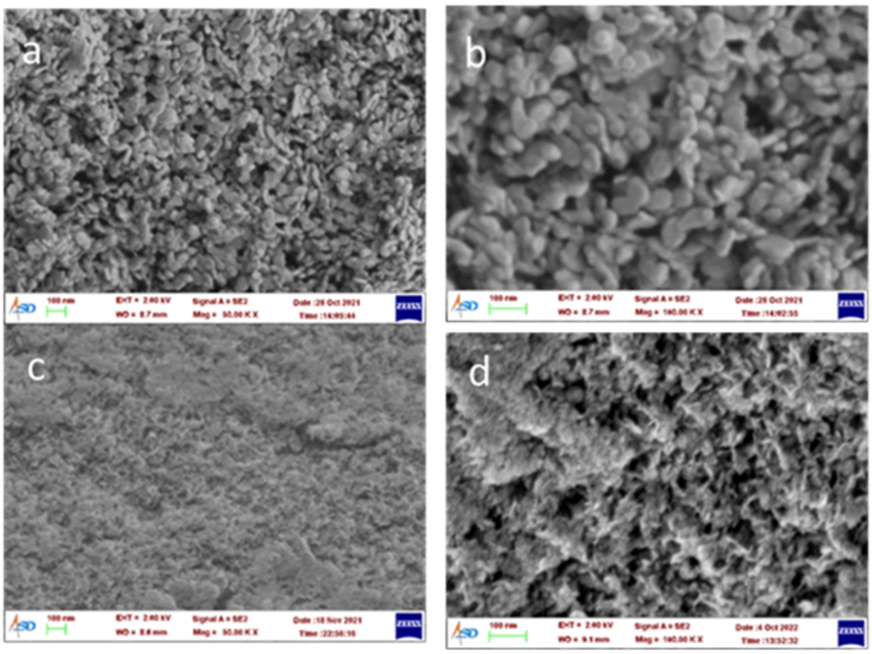

Fig.S7 FESEM images of (a, b) CoAl-31 LDH and (c, d) NiAl-31 LDH

Table S_3 Comparison of Magnetically separable catalysts for PET glycolysis

	Catalyst	BHET yield (%)	Temperature	Time (H)	Reference
1	Superparamagneti	90	300, 1.1 MPa	1	https://doi.org/10.1039/C3G

	c γ-Fe2O3 Nanoparticles				C41834K
2	γ-Fe_2O_3/nitrogen-doped graphene hybrid material	100	195	3	http://dx.doi.org/10.1016/j.polymdegradstab.2017.08.033
3	Fe3O4@SiO2@(mim)[FeCl4]	63	170	24	https://doi.org/10.1016/j.apcatb.2019.118110
4	γ-Fe_2O_3	40	195	3	http://dx.doi.org/10.1016/j.polymdegradstab.2017.08.033
5	h-BNNS with Fe3O4 nanoparticles	100	200, in autocalve		https://doi.org/10.1016/j.polymdegradstab.2019.108962
6	Fe_3O_4-boosted MWCNT	100	190	2	https://doi.org/10.1039/C6GC00534A.
7	ZnO–Fe_3O_4 magnetic hollow micro-sized nanoaggregates	92.3	190	0.5	https://doi.org/10.1039/D3GC01762A
8	Mg-Al-O@Fe3O4	31.4	240	1.5	https://doi.org/10.1016/j.wasman.2021.03.049
9	two-dimensional FeIII nanosheets	100	200	0.5	https://doi.org/10.1039/D0RE00385A
10	Fe3O4 nanodispersions	93	210	0.5	https://doi.org/10.1021/acssuschemeng.3c01206
11	Fe3O4-CP	93.5	190	2	https://doi.org/10.1039/D3GC01707A
12	Coal @Fe3O4	99	180	2	This work

Table S_4 ICP-AES analysis of Co-Al 31@Fe_3O_4

Element	Wt.% (from ICP-AES)
Cobalt	29.8
Aluminum	4.7
iron	18.2